Combinatorial CRISPR screen reveals *FYN* and *KDM4* as targets for synergistic drug combination for treating triple negative breast cancer

Running title: FYN and KDM4 inhibition synergizes with TKIs

Tackhoon Kim[1,2,3,4,*] Byung-Sun Park[1,2], Soobeen Heo[5], Heeju Jeon[1,2], Jaeyeal Kim[1,2], Donghwa Kim[6], Sang Kook Lee[6], So-Youn Jung[7], Sun-Young Kong[5,8], Timothy K. Lu[4,*]

[1] Medicinal Materials Research Center, Korea Institute of Science and Technology, 5 Hwarangro-14-gil, SeongbukGu, Seoul 02792, Republic of Korea

[2] Department of Biological Sciences, Korea University, 145 AnamRo, SeongbukGu, Seoul 02841, Republic of Korea

[3] Division of Bio-Medical Science and Technology, Korea University of Science and Technology, 217 GajeongRo YuseongGu, Daejeon 34113, Republic of Korea

[4] Research Lab of Electronics, Massachusetts Institute of Technology, 77 Massachusetts Avenue, Cambridge MA 02139, USA

[5] Targeted Therapy Branch, Division of Rare and Refractory Cancer, Research Institute, National Cancer Center, Goyang 10408, Korea

[6] College of Pharmacy, Natural Products Research Institute, Seoul National University, 1 Gwanakro, Gwanakgu, Seoul 08826, Republic of Korea.

[7] Division of Breast Surgery, Department of Surgery, National Cancer Center, Goyang 10408, Korea

[8] Department of Laboratory Medicine, National Cancer Center, Goyang 10408, Republic of Korea

*** Correspondence**: Tackhoon Kim, 5 Hwarangro-14-gil, SeongbukGu, Seoul 02792, Republic of Korea;

Timothy K. Lu, 500 Technology Square, Cambridge MA 02139, USA.

Email: tackhoon@kist.re.kr; tim@lugroup.org

Competing Interest Statement

The authors declare no conflict of interest

Abstract

Tyrosine kinases play a crucial role in cell proliferation and survival and are extensively investigated as targets for cancer treatment. However, the efficacy of most tyrosine kinase inhibitors (TKIs) in cancer therapy is limited due to resistance. In this study, we identify a synergistic combination therapy involving TKIs for the treatment of triple negative breast cancer. By employing massively parallel combinatorial CRISPR screens, we identify *FYN* and *KDM4* as critical targets whose inhibition enhances the effectiveness of TKIs, such as NVP-ADW742 (IGF-1R inhibitor), gefitinib (EGFR inhibitor), and Imatinib (ABL inhibitor) both *in vitro* and *in vivo*. Mechanistically, treatment with TKIs upregulates the transcription of *KDM4*, which in turn demethylates H3K9me3 at *FYN* enhancer for *FYN* transcription. This compensatory activation of *FYN* and *KDM4* contributes to the resistance against TKIs. We highlight *FYN* as a broadly applicable mediator of therapy resistance and persistence by demonstrating its upregulation in various experimental models of drug-tolerant persisters and residual disease following targeted therapy, chemotherapy, and radiotherapy. Collectively, our study provides novel targets and mechanistic insights that can guide the development of effective combinatorial targeted therapies, thus maximizing the therapeutic benefits of TKIs.

Introduction

Tyrosine kinases have emerged as important drug targets in cancer therapy due to their druggability and pivotal roles in cell proliferation and survival(1). They are implicated in various aspects of cancer development(2), such as cell survival, proliferation, angiogenesis, and invasion, making them attractive targets for drug intervention. Consequently, tyrosine kinase inhibitors (TKIs) have gained considerable attention as primary agents for cancer treatment.

Triple negative breast cancer (TNBC) treatment has limited options for targeted therapy. TNBC, characterized by the absence of estrogen receptor, progesterone receptor, and HER2 expression, exhibits elevated activity of tyrosine kinases, including EGFR and IGF1R(3, 4). However, several clinical trials investigating TKIs, such as VEGFR inhibitors, EGFR inhibitors, and FGFR inhibitors, in TNBC treatment have yielded disappointing results due to inadequate efficacy. Therefore, it is crucial to comprehend the mechanisms underlying TNBC's suboptimal response to TKIs to enable the development of more effective targeted therapies against TNBC.

The therapeutic efficacy of TKIs is compromised by intrinsic and acquired resistance(5). For instance, EGFR inhibitor gefitinib extended the median progression-free survival by only five months compared to conventional

chemotherapy in non-small cell lung cancer (NSCLC) patients with EGFR mutation(6). Significant subset of drug resistance is driven by gene interactions that enable compensatory changes in signal transduction upon drug treatment. Compensatory activation of mitogenic signals, such as MET, PIK3CA amplification, and MAPK/ERK signaling activation, counterbalances the inhibition of EGFR by TKI osimertinib in a significant portion of NSCLC patients(7). Simultaneous inhibition of multiple signaling molecules that compensate for each other's loss is proposed as an effective strategy to overcome resistance to kinase inhibitor therapy, emphasizing the importance of combinatorial therapy(8).

Until recently, a highly scalable method for screening combinatorial therapy has been lacking. Combinatorial CRISPR screens have emerged as efficient tools to identify synergistic targets for combinatorial therapy. We and others recently developed massively parallel combinatorial CRISPR screens to elucidate pairwise gene interactions(9-12). Our combinatorial genetic screen platform, combinatorial genetics *en Masse* (combiGEM), was successfully implemented to identify combinations of epigenetic regulators causing synthetic lethality in ovarian cancer cells (9).

In this study, we utilize CombiGEM-CRISPR technology to identify synergistic tyrosine kinase inhibitor combinations for effective elimination of TNBC. We highlight FYN as a key therapeutic target that, when inhibited, enhances the cytotoxic effect of inhibition of other tyrosine kinases (IGF1R, EGFR, and ABL2). Mechanistic studies reveal KDM4 as a crucial epigenetic regulator that demethylates H3K9me3 and transcriptionally upregulates *FYN* upon TKI treatment. *In vitro* and *in vivo* validation demonstrates the synergistic TNBC-shrinking effects of combining PP2, saracatinib (FYN inhibitor) or QC6352 (KDM4 inhibitor) with TKIs. Additionally, we demonstrate the clinical significance of our findings by observing upregulation of *FYN* in various models of drug tolerant persisters and residual tumors after chemo-, radio-, or targeted therapy. Therefore, simultaneous targeting of *FYN-KDM4* and tyrosine kinase pathways through combinatorial therapy holds promise for effective therapy against TNBC.

Results

For efficient translation of CRISPR screening data to drug combination, we selected 76 tyrosine kinases that could be inhibited by at least one drug from the drug repurposing hub database (table S1) (13). For pairwise CombiGEM library construction, we chose three guide RNAs from the optimized Brunello sgRNA list(14)

employing the iterative cloning method as previously described(9, 15). The resulting library enabled massively parallel screens of pairwise knockouts, encompassing 54,289 sgRNA pairs representing 3,003 pairwise gene disruptions (Fig. 1A). To validate our library, we performed next-generation sequencing and confirmed that 99.5% (2,989/3,003) of gene pairs were represented by at least 6 pairs of sgRNAs, with the $\log_{10}$ reads per million of 0.5 (Fig. S1A).

Triple negative breast cancer cell line MDA-MB-231 cells stably expressing Cas9 were infected with the lentiviral library at low multiplicity of infection (MOI) of 0.3. Genomic DNA was harvested 3 days after infection (designated as day 0[D0]), and 23 days after infection (D20) (Fig. 1A) to perform PCR amplification of sgRNA pairs for subsequent next-generation sequencing (NGS) analysis. Our previous CombiGEM screens, involving the sequencing of contiguous stretches of barcodes for sgRNAs, did not accurately reflect the combinations of sgRNAs expressed in cells due to the uncoupling of sgRNA and barcodes during lentiviral replication and reverse transcription(16). In fact, the decoupling rate of barcode from sgRNA increased with the distance between them, reaching ~35% in pairwise screens (Fig. S1B). To address this issue, we directly sequenced the sgRNA spacer sequences using paired-end sequencing (Fig. S1C). We counted the occurrences of each sgRNA pair in the NGS data and calculated the normalized log2 fold change in counts between the day 20 and day 0 samples as the growth phenotype score Z (see Methods). The counts for the two permutations of an sgRNA pair (e.g., sgRNA-A + sgRNA-B and sgRNA-B + sgRNA-A) exhibited good correlations (r = 0.50) and were combined when calculating Z (Fig. S1D). The Z scores for three biological replicates also demonstrated strong correlations (r = 0.74 between replicates #2 and #3) (Fig. S1E). Additionally, we confirmed that independent sgRNA pairs targeting the same set of genes showed correlated changes in the growth phenotype (Fig. S1F-G).

We aimed to identify gene perturbations that exhibit synergistic cell-killing effects by calculating gene interaction scores (GI). The GI scores were derived by comparing the growth phenotype score Z resulting from the disruption of a gene pair (Z_{A+B}, observed Z score) to the sum of Z scores obtained from the disruption of each gene individually within the pair ($Z_{A+Con} + Z_{B+Con}$, expected Z score). We computed GI scores at both the sgRNA level and the gene level. At the gene level, we employed the Z scores of all sgRNA pairs targeting the same gene pair to calculate the gene interaction score (GI), as demonstrated in Figure 1B. The expected and observed Z scores for each gene (or sgRNA) pair exhibited a strong positive correlation, as shown in Figure 1B for gene level analysis and Figure S1H for sgRNA level analysis. This correlation suggests that most random

pairwise combinations of tyrosine kinase perturbations have merely additive effects on cancer cell killing, as expected. To calculate the GI scores, we normalized the observed Z score by quantifying its deviation from the quadratic fit of the expected-observed Z score plot(10). The GI scores were normalized (Fig. 1C) by dividing them by the standard deviation of the GI scores obtained from the 200 nearest neighbors in terms of expected Z scores. The standard deviation of the raw GI scores tend to increase at extremely low expected Z scores as previously reported(11) (Fig. S1I).

Using cutoffs for gene level GI score <-2 and p<0.01 for GI scores determined by RIGER analysis(17) and Z<-5 (Fig. 1D and dataset S1), we selected thirty synthetic lethal gene pairs. Among these, the SRC-YES pair exhibited one of the strongest synthetic lethal gene pairings (GI= -3.95). Notably, SRC-YES belong to the same tyrosine kinase family and are known to be functionally redundant and are expected to be synthetic lethal(18). These findings provide evidence for the effectiveness of our screening approach in identifying synthetic lethal gene pairs.

We subsequently conducted validation experiments to confirm the occurrence of synergistic cell death in the candidate synthetic lethal pairs. To achieve this, we introduced lentiviral vectors carrying two distinct single-guide RNAs (sgRNAs) targeting the candidate synthetic lethal pairs, each tagged with a different fluorescent protein (GFP and mCherry). MDA-MB-231-Cas9 cells were infected with the lentivirus at a low titer (MOI ~0.5), resulting in a mixed population of cells expressing either one or both sgRNAs along with their respective fluorescent proteins (Fig. 2A). To evaluate synthetic lethality, we monitored the progressive decrease in the number of GFP/mCherry double-positive cells over time (see methods). We validated the efficacy of the sgRNAs used in Figure 2A through the T7 endonuclease assay, which confirmed efficient gene editing (Fig. S2A). Consistent with our CRISPR screening results, we observed that the disruption of six out of eight synergistic target gene combinations led to a reduction in cell viability beyond what was predicted by the Bliss independence model (Fig. 2B). Moreover, the relative viability of double knockout cells and the rate of synergistic killing demonstrated a strong correlation with our screening data (r = 0.65 for both viability and synergistic effect; Fig. S2B). Collectively, our findings provide compelling evidence that our screening approach successfully identified synthetic lethal gene pairs with a high level of confidence.

During our analysis, we observed that several validated synergistic target gene pairs included *FYN* (e.g. *FYN*+IGF1R, *FYN*+EGFR, and *FYN*+ABL2). Notably, network analysis of the 30 candidate synergistic tyrosine

kinase pairs revealed that *FYN* is one of the key nodes participating in synergistic interactions with multiple genes (Fig. 2C). Interestingly, we found that *FYN*, but not SRC, exhibited significant upregulation in triple-negative breast cancer (TNBC) compared to other subtypes, as evidenced by microarray data from primary tumor samples (19) and the cancer cell line encyclopedia (CCLE)(20) (Figs. 2D-E). These findings suggest that gene A could represent an attractive drug target for TNBC treatment. To investigate this further, we assessed whether simultaneous inhibition of FYN by PP2, which selectively targets the SRC family kinase inhibitor with the highest potency against FYN, in combination with other kinase inhibitors (TKIs), could inhibit cancer cell growth(21). Intriguingly, analysis using SynergyFinder(22) revealed that all TKI combinations involving PP2 and NVP-ADW742 (IGF1R inhibitor), gefitinib (EGFR inhibitor) or Imatinib (ABL inhibitor) synergistically induced cell death in MDA-MB-231 cells (Fig. 2F). Dose-response curves demonstrated that co-treatment with PP2 reduced the IC50 of the tested TKIs by 34-61%, indicating that PP2 sensitized cancer cells to TKI treatment (Fig. 2G). Similar synergy was observed when TKI combinations included saracatinib in place of PP2 (Fig. S3A). Moreover, specific ablation of *FYN*, but not SRC, sensitized cells to TKIs, highlighting the critical role of FYN as a member of SRC kinase family responsible for TKI resistance (Figs. 2H and S3B). Importantly, we observed similar synergy between the same drug combinations in other TNBC cell lines, including Hs578T, HCC1143, HCC1395, and HCC1937 cells (Fig. S3C-F). Further assessment using live-dead and BrdU assays revealed that both the PP2+NVP-ADW742 and PP2+gefitinib combinations synergistically induced cell death while inhibiting cell growth (Fig. 2I).

Persistent activation of MAPK pathway and PI3K-AKT pathway has been associated with TKI resistance in various cancers(5). Therefore, we investigated which downstream pathways were involved in sensitizing cells to TKI treatment. Notably, the p38 MAPK was significantly attenuated following treatment with either PP2 or saracatinib treatment (Fig. 2J). Genetic ablation of *FYN* similarly reduced p38 activation (Fig. 2K). Attenuation of p38 activity was also observed in an independent TNBC cell line, Hs578T (Figs. S3G-H). Importantly, treatment of p38 MAPK pathway inhibitor SB203580 markedly sensitized cells to TKI treatment (Fig. 2L).

Our discovery that inhibition of FYN synergizes with multiple TKIs possessing distinct target profiles suggests that FYN may play a role in general resistance mechanisms against TKI therapy. Consistently, we observed an increase in both protein and mRNA levels of *FYN* following TKI treatment, indicating that upregulation of FYN confers compensatory survival signal in TKI-treated cells (Fig. 3A-B). To elucidate the mechanisms underlying the accumulation of *FYN*, we treated MDA-MB-231 cells with inhibitors targeting key epigenetic modifiers and

assessed their synergistic effects with NVP-ADW742 in cell killing, as well as their impact on *FYN* mRNA accumulation. Intriguingly, we found that GSK-J4, an inhibitor of the jumonji domain histone demethylase family (23), was the only drug in our initial screen that decreased *FYN* mRNA and viability upon TKI treatment (Figs. S4A-B). Furthermore, treatment with NVP-ADW742 increased the expression of most members of the jumonji domain histone demethylase family (Fig. 3C). This observation is consistent with a previous study on taxane-resistant H1299 lung cancer cells(24), suggesting that histone demethylases may play critical roles in activating a drug resistance gene program. However, the ablation of KDM6, the primary targets of GSK-J4, failed to significantly decrease *FYN* expression (Fig. S4C). GSK-J4 is known to inhibit other jumonji domain histone demethylase family proteins including KDM4 and KDM5(25). Therefore, we tested the possibility that other histone demethylase may be involved in regulating *FYN* expression. Among jumonji domain histone demethylases, *KDM4*, and to a lesser extent *KDM3*, were the only gene family members whose ablation inhibited *FYN* upregulation and p38 activation upon TKI treatment (Figs. 3D and S4D). Ablation of KDM5, which has been shown to induce drug tolerance in cancer cells(26), did not significantly alter *FYN* expression (Fig. S4E). Similar to NVP-ADW742 treatment, gefitinib treatment increased *KDM4* demethylase levels (Fig. S4F). We also analyzed two independent TNBC organoids obtained from primary tumors and found concurrent upregulation of *KDM4* with *FYN* mRNAs upon NVP-ADW742 and gefitinib treatment (Fig. S4G). Both KDM3 and KDM4 demethylates methylated H3K9, thereby promoting the opening heterochromatin for transcription(27). Remarkably, *KDM4A* expression was upregulated in TNBC (Fig. 3E) and exhibited a positive correlation with *FYN* expression in CCLE database, suggesting that KDM4 regulates *FYN* mRNA levels (Fig. 3F). Genetic ablation of *KDM3* or *KDM4* (Fig. S5A) decreased *FYN* and p38 activity, sensitizing MDA-MB-231 cells to TKIs (Figs. 3G-H). Likewise, treatment of KDM4 inhibitor QC6352(28) synergized with TKIs in killing MDA-MB-231 cells (Fig. 3I). QC6352 treatment also significantly attenuated *FYN* accumulation upon NVP-ADW742 treatment (Fig. 3J-K). This was consistent with the RNA sequencing data results in the previous study with breast cancer stem cells treated with QC6352(29). Specifically, *FYN* was the most significantly downregulated SRC family kinase upon QC6352 treatment among (Fig. 3L). Analysis of chromatin IP (ChIP) sequencing data from the same study revealed KDM4A enrichment near FYN promoter; and QC6352 treatment increased H3K9me3 enrichment at the same locus (Fig. 3M). Indeed, this FYN promoter locus exhibited a reduction in H3K9me3 following NVP-ADW742 treatment, while QC6352 treatment restored H3K9me3 enrichment (Fig. 3N). This finding suggests that KDM4 may directly demethylate H3K9me3 at FYN promoter to upregulate *FYN* transcription. *FYN* accumulation and resistance to TKIs were also confirmed to be attenuated

by QC6352 treatment in other independent TNBC cell lines (Figs. S5B-C).

We proceeded to investigate the potential clinical application of our synthetic lethal gene pairs as combinatorial therapy by assessing the *in vivo* efficacy of pharmacological interventions targeting these gene pairs using MDA-MB-231 xenograft models. Strikingly, co-treatment of saracatinib and NVP-ADW742 synergistically reduced tumor size, whereas treatment with either agent alone was ineffective in slowing tumor growth (Fig. 4A). All treatment groups exhibited minimal changes in body weight, indicating that the overall health of the animals was not adversely affected by the combination treatment (Fig. S6A). Saracatinib-gefitinib combination was not tested as saracatinib can inhibit EGFR(30). Similarly, KDM4 inhibitor QC6352 synergized with gefitinib in reducing MDA-MB-231 xenograft tumor growth without causing overt changes in animal health (Figs. 4B and S6B). Additionally, the expression levels of *FYN* and *KDM4A* were found to be correlated with poor prognosis in a previously reported breast cancer cohort(19), highlighting the potential of targeting these two genes as therapeutic targets for TNBC (Fig. 4C Collectively, our results demonstrate that upregulation of *KDM4* upon TKI treatment reduces H3K9me3 mark in *FYN* enhancer, thereby increasing *FYN* expression and promoting cell survival under TKI treatment (Fig. 4D).

The observed epigenetic alterations in regulators conferring resistance to multiple cancer drugs closely resemble non-genetic changes associated with the generation of drug-tolerant persisters(26). Indeed, prolonged incubation of MDA-MB-231 cells treated with TKIs or conventional chemotherapy drugs such as doxorubicin or paclitaxel resulted in increased levels of *FYN* (Fig. 5A). Curiously, *KDM4A* expression was only upregulated upon treatment with NVP-ADW742 and gefitinib, suggesting that while *FYN* upregulation is a general feature of drug tolerant cells, the mechanism of *FYN* upregulation may vary depending on the specific drug being used. Analysis of previously published RNA sequencing data from a series of Osimertinib tolerant EGFR mutated lung cancer cell lines(31) revealed higher expression levels of *FYN* and *KDM4A* in the drug persisters, but not SRC (Fig. 5B). Consistently, we confirmed upregulation of *FYN* at both the protein and mRNA levels in gefitinib and osimertinib resistant PC9 and HCC827 cells (Figs. 5C-D). Pharmacological inhibition of FYN or downregulation of *FYN* expression through inhibition of KDM4 sensitized gefitinib resistant PC9 cells to EGFR inhibitor, suggesting that *FYN-KDM4* are responsible for gefitinib resistant phenotype in this cell line (Figs.5E-G).

Importantly, upregulation of *FYN* has been consistently observed in multiple independent studies involving

drug-tolerant cancer cell lines and patient-derived xenografts treated with various drugs that have distinct target profiles, including TKIs (e.g., lapatinib, a HER2 inhibitor) and chemotherapy drugs (e.g., irinotecan) (Fig. 5H). Moreover, enrichment of *FYN* has also been observed in residual disease following chemotherapy, indicating its potential role in mediating drug tolerance during chemotherapy (Fig. 5I). Notably, an analogous increase in *KDM4* was not consistently observed across all tumor models tested in Figures 5H-I (Fig. S7A-B). This suggests that, as previously noted in Figure 5A, while *FYN* serves as a general mediator of drug tolerance, the specific mechanisms underlying its upregulation may vary depending on the cancer type and the drug being administered. Taken together, these lines of evidence further support our findings in TNBC cell lines and suggest that *FYN* acts as a common mediator of drug tolerance.

Discussion

In this study, we employed massively parallel, combinatorial CRISPR screening to identify combinations of TKIs that exhibit synergistic effects in eliminating triple-negative breast cancer (TNBC). We discovered and validated that concurrent targeting of FYN, along with other tyrosine kinases such as IGF1R, EGFR or ABL2 can synergistically eradicate TNBC and impede cancer growth. Our findings also provide evidence that the transcriptional upregulation of *FYN*, facilitated by the activation of KDM4 histone demethylases, confers resistance and persistence to TKIs. Upregulation of *FYN* is a general feature of drug tolerant cancer cells, suggesting *FYN* as an attractive target for minimization of tumor recurrence after treatment.

This research provides basis for breakthrough combinatorial therapy achieving effective targeted therapy with minimal risk of developing resistance. Our combinatorial CRISPR screening demonstrates that treatment with TKIs or histone demethylase inhibitors enhances the sensitivity of cells to other TKIs. Consequently, drug combinations exhibit a more potent inhibition of cancer growth than the simple sum of the therapeutic effects of individual drugs. Furthermore, synergistic drug combinations enable a reduction in the dosage of each drug, with minimal compromise in therapeutic efficacy. Such combinations yield a therapeutic response comparable to that achieved with significantly higher doses of each individual agent. We anticipate that combinatorial therapy has the potential to mitigate side effects by minimizing the dosage of each drug, thus widening the therapeutic window.

Additionally, our work underscores the potential utility of kinase inhibitors with promiscuous binding profiles.

Most kinase inhibitors target the highly conserved ATP binding pocket, resulting in multiple target interactions(32). While substantial efforts have been made to enhance the specificity of kinase inhibitors, the repurposing of inhibitors with more relaxed specificity as dual or multi-kinase inhibitors, targeting synergistic kinase targets, may offer therapeutic advantages. The rational design of dual kinase inhibitors holds significant promise for advancing therapeutic interventions.

It is intriguing to observe that *FYN* is specifically upregulated in various models of drug resistance and tolerance. While other SRC family kinases have been linked to drug resistance(33), the precise molecular mechanisms underlying their increased contribution to cell survival upon drug treatment remained unclear. Our findings reveal that *FYN* is specifically upregulated at the mRNA level through epigenetic regulations, providing further depth to our understanding of drug resistance in cancer therapy.

Furthermore, our work highlights the significance of histone demethylases in TKI resistance. Numerous histone demethylases have been implicated in drug resistance and tolerance across different cancer drug types. For instance, the KDM5 family of H3K4 demethylases has been associated with the drug-tolerant persister phenotype against multiple TKIs(26). In our study, we identify *KDM4* as a critical factor in the generation of drug-tolerant persisters in breast cancer. *KDM4* is known to be upregulated in various cancers, including breast cancer, and promotes key malignant traits. Previous studies have demonstrated the essential role of KDM4 in induced pluripotency through its interaction with pluripotency factors(34). These findings suggest that an KDM4 inhibitor could be a promising therapeutic target with specific activity against cancer stem cells. Consistently, specific inhibitors targeting KDM4 have recently been developed and shown to inhibit the generation of breast cancer stem cells(29). Given our discoveries regarding the involvement of *KDM4* in drug resistance in breast and lung cancer, the development of novel drugs targeting KDM4 holds significant therapeutic potential.

Materials and methods

Cell Culture. HEK293T, MDA-MB-231, Hs578T cells were obtained from American Type Cell Culture (ATCC) HCC1143, HCC1395, HCC1937 were obtained from Korean cell line bank. HEK293T and MDA-MB-231were grown in DMEM (Gibco) supplemented with 10% FBS (Corning) and penicillin/streptomycin (Gibco). Hs578T and HCC1143, HCC1395, HCC1937 were grown in RPMI1640 (Gibco) supplemented with 10% FBS.

Combinatorial library construction. Combinatorial library was constructed as previously described(15). The

sgRNAs used in the screens were cloned in pAWp28 storage vector in two versions: one version containing human U6 driven sgRNA with wild type scaffold, and another containing mouse U6 driven sgRNA with cr2 variant scaffold. The sgRNA expression cassette consisting of U6 promoter and sgRNA were subject to one-pot, iterative cloning into lentiviral pTK799 vector using BglII-MfeI restriction sites flanking the sgRNA expression cassette and BamHI-EcoRI sites in pTK799. pTK799 vector is derived from pAWp12(15) by replacing CMV-GFP selectable marker to EFS-Puro.

Combinatorial CRISPR screening procedure. Lentivirus was generated in HEK293T cells by transfecting lentiviral transfer vector, and helper vectors (psPAX2, and pVSV-G) using Fugene HD (Promega). Lentiviral supernatant was collected 48 hours after transfection, and was frozen and stored in -80C. The appropriate titer for lentiviral infection was determined by infecting MDA-MB231 cells with two-fold serial dilution of lentiviral supernatant, selecting with puromycin 2 days after infection for 2 days, and determining cell viability with AQuaeous one cell viability, MTS assay (Promega). After determining the titer of lentiviral supernatant, 100 million MDA-MB231 cells carrying constitutively expressed Cas9 were infected with CombiGEM library at MOI of 0.3. The expected initial coverage is 100 million x 0.3/ (54,289 different sgRNA combinations)= 553. Three days after infection, the infected cells were either harvested as day 0 sample or selected with 2ug/mL puromycin. Cells were treated with benzonase before harvesting to minimize carryover of plasmid DNA in lentiviral supernatant. Cells were grown in the presence of 2µg/mL puromycin for 20 days before havesting.

The genomic DNA of harvested cells were isolated using Blood & Cell Culture Maxi kit (Qiagen). The PCR amplicon spanning the two sgRNAs were generated with PCR using Q5 High Fidelity DNA polymerase (New England Biolabs) and the following primers:

F: CAAGCAGAAGACGGCATACGAGAT CCTAGTAACTATAGAGGCTTAATGTGCG

R: AATGATACGGCGACCACCGAGATCTACAC NNNNNN ACACGAATTCTGCCGTGGATCCAA

The six variable nucleotides were added in reverse primer for multiplexing.

The PCR protocols involves 60 seconds of initial DNA denaturation at 98C, and 20 cycles of 10 seconds denaturation at 98C, 10 seconds annealing at 67C, and 120 seconds elongation at 72C. All genomic DNA isolated were used in PCR reaction at concentration of 40ug/mL. All PCR products were combined and precipitated with isopropanol at room temperature. The precipitated DNA was resuspended in 400uL EB buffer

(Qiagen) and gel purified. The purified PCR products were sent for NGS by NextSeq500 paired end sequencing with the following sequencing primers:

Forward read: GGACTAGCCTTATTTGAACTTGCTATGCAGCTTTCTGCTTAGCTCTCAAAC

Forward index read: CGGTGCCACTTTTTCAAGTTGATAACGGACTAGCCTTATTTTAACTTGCTATTTCTAGCTCTAAAAC

Reverse read: GCA CCG AGT CGG TGC TTT TTT GGA TCC ACG GCA GAA TTC GTGT

Data analysis. The sgRNA sequences were identified and their occurrences were counted with C++ script deposited in Github (https://github.com/tackhoonkim/combinatorial-CRISPR-screens-2023).

Validation of screens using sgRNAs. Individual sgRNA was cloned to either pTK1329, and pTK1336 that are both derived from pAWp12 with EFS-GFP and EFS-mCherry, respectively, as selectable markers. Validation of synthetic lethality between gene A and B were analyzed by infecting MDA-MB-231 Cas9 cells with four combinations of lentiviral supernatant pairs (MOI ~ 0.5 each) containing (1) GFP-sgA and mCherry-sgB; (2) GFP-sgA and mCherry-sgCon; (3) GFP-sgCon and mCherry-sgB; (4) GFP-sgCon and mCherry-sgCon. The fraction of GFP/mCherry double positive cells were analyzed using BD Accuri C6 and its accompanying software. The expected fold change in sgA+sgB were calculated as $FC_{sgA+sgCon}$ x $FC_{sgCon+sgB}$, where FC is normalized fold change in fraction of GFP/mCherry double positive cells relative to those infected with GFP-sgCon and mCherry-sgCon.

MTT Cell viability assay. Cells were seeded at 1000-2000 cells/well in 96 well plate. Tyrosine kinase inhibitors at indicated combination of dose were treated 12 hours after seeding, and cells were grown for 3 days. The relative viability was measured by EzCytox cell viability assay (Dojindo). The absorbance at 450nm wavelength was measured using EnVision multimode plate reader (PerkinElmer).

Cell death and cell proliferation assay. Cells were incubated with tyrosine kinase inhibitors for 48 hours. Cell proliferation was quantified with BrdU assay using FITC conjugated BrdU antibody (Biolegend) and propidum iodide/RNase A solution (Cell Signaling), analyzed with BD Accuri C6 and accompanied software. Cell death was quantified with Live-Dead cell staining kit (Molecular Probes) by flow cytometry analysis using BD Accuri C6 and accompanied software.

Western blot analysis. Cells were treated with drugs for 48 hours unless otherwise indicated. Cells were lysed in RIPA buffer supplemented with protease inhibitor and phosphatase inhibitor cocktail. Antibodies used for western blot analysis were all from Cell Signaling Technology. The original blot scans are available in figure S8.

Xenograft assay. All animal experiments were approved by IACUC of Korea Institute of Science and Technology (KIST). Six week old female nude mice were injected with 5 x 10^6 MDA-MB-231 cells suspended in 1:1 (w/w) mixture of PBS and growth factor reduced Matrigel (Corning) in fourth inguinal mammary fat pad. Starting two weeks after tumor cell injection, saracatinib (50mg/kg mouse body weight), NVP-ADW742 (20mg/kg), gefitinib (20mg/kg), QC6352 (10mg/kg) in 45% saline+40% polyethyleneglycol 300 (sigma)+5% Tween-80 (sigma)+5% DMSO (sigma) were injected intraperitoneally every 24 hours for two weeks. Tumor volume was measured by digital caliper and calculated as $(\text{width})^2$ x length x 0.5.

Public database analyses. Gene Expression Omnibus (GEO) data with breast cancer cohort (GSE25066(19)) were analyzed using web based platform Cancer Target Gene Screening (https://ctgs.biohackers.net)(35). Cancer Cell Line Encyclopedia (CCLE) data were analyzed using depmap R package version 1.14. The list of GEO data used for analysis are listed in table S2.

Primary TNBC organoid culture and drug treatment. Tumor tissue were collected in breast cancer at the National Cancer Center (Goyang, Republic of Korea) with IRB approval. After additional refining steps and cell counting, 1×10^5 cells were embedded in 50 µl of Matrigel (Corning, NY, USA) and seeded in each well of a 24-well cell culture plate. After the matrigel was solidified, 500 µL medium supplemented with defined growth factors as described by Clevers and colleagues(36), was added to each well and grown under standard culture conditions (37 ℃, 5% CO2).

Acknowledgments.

We thank BioMicro Center of MIT for sequencing analysis. We thank Jae Cheol Lee (Asan Medical Center, Korea) for providing gefitinib resistant lung cancer cell lines. This work was supported by Korea Institute of Science and Technology (KIST) Institutional Programs (2E32331 to T.K.); and National Research Foundation of Korea, funded by the Korean government (MSIT) (2021R1A2C1093499 to T.K., 2020M3A9A5036362 to S.Y.K).

Author contributions. T.K., B.-S.P., H.J. and J.K. performed experiments. T.K. and T.K.L. supervised the

research. S.H. S.-Y.J. and S.Y.K. performed experiments with TNBC patient derived organoids. D.K., S.K.L. generated and provided Osimertinib resistant HCC827 cell line.

Conflict of Interest Statement

The authors declare no conflict of interest

Ethics Statement

All experiments with human tumor organoids were conducted in accordance with the requirements of the National Cancer Center Inatitutional Review Board (IRB).

Availability of data and materials: The NGS data for CRISPR screening results are available under NCBI SRA accession code PRJNA976939.

References

1. Wu P, Nielsen TE, Clausen MH. Small-molecule kinase inhibitors: an analysis of FDA-approved drugs. Drug Discovery Today. 2016;21(1):5-10.
2. Hanahan D, Weinberg Robert A. Hallmarks of Cancer: The Next Generation. Cell. 2011;144(5):646-74.
3. Li Y, Zhan Z, Yin X, Fu S, Deng X. Targeted Therapeutic Strategies for Triple-Negative Breast Cancer. Frontiers in Oncology. 2021;11.
4. Litzenburger BC, Creighton CJ, Tsimelzon A, Chan BT, Hilsenbeck SG, Wang T, et al. High IGF-IR Activity in Triple-Negative Breast Cancer Cell Lines and Tumorgrafts Correlates with Sensitivity to Anti–IGF-IR Therapy. Clinical Cancer Research. 2011;17(8):2314-27.
5. Morgillo F, Della Corte CM, Fasano M, Ciardiello F. Mechanisms of resistance to EGFR-targeted drugs: lung cancer. ESMO Open. 2016;1(3):e000060.
6. Maemondo M, Inoue A, Kobayashi K, Sugawara S, Oizumi S, Isobe H, et al. Gefitinib or Chemotherapy for Non–Small-Cell Lung Cancer with Mutated EGFR. New England Journal of Medicine. 2010;362(25):2380-8.
7. Leonetti A, Sharma S, Minari R, Perego P, Giovannetti E, Tiseo M. Resistance mechanisms to osimertinib in EGFR-mutated non-small cell lung cancer. British Journal of Cancer. 2019;121(9):725-37.
8. Jin H, Wang L, Bernards R. Rational combinations of targeted cancer therapies: background, advances and challenges. Nature Reviews Drug Discovery. 2023;22(3):213-34.
9. Wong ASL, Choi GCG, Cui CH, Pregernig G, Milani P, Adam M, et al. Multiplexed barcoded

392 CRISPR-Cas9 screening enabled by CombiGEM. Proceedings of the National Academy of Sciences.
393 2016;113(9):2544-9.
394 10. Horlbeck MA, Xu A, Wang M, Bennett NK, Park CY, Bogdanoff D, et al. Mapping the
395 Genetic Landscape of Human Cells. Cell. 2018;174(4):953-67.e22.
396 11. Han K, Jeng EE, Hess GT, Morgens DW, Li A, Bassik MC. Synergistic drug combinations for
397 cancer identified in a CRISPR screen for pairwise genetic interactions. Nature Biotechnology.
398 2017;35(5):463-74.
399 12. Shen JP, Zhao D, Sasik R, Luebeck J, Birmingham A, Bojorquez-Gomez A, et al.
400 Combinatorial CRISPR–Cas9 screens for de novo mapping of genetic interactions. Nature Methods.
401 2017;14(6):573-6.
402 13. Corsello SM, Bittker JA, Liu Z, Gould J, McCarren P, Hirschman JE, et al. The Drug
403 Repurposing Hub: a next-generation drug library and information resource. Nature medicine.
404 2017;23(4):405-8.
405 14. Doench JG, Fusi N, Sullender M, Hegde M, Vaimberg EW, Donovan KF, et al. Optimized
406 sgRNA design to maximize activity and minimize off-target effects of CRISPR-Cas9. Nature
407 Biotechnology. 2016;34(2):184-91.
408 15. Wong ASL, Choi GCG, Cheng AA, Purcell O, Lu TK. Massively parallel high-order
409 combinatorial genetics in human cells. Nat Biotech. 2015;33(9):952-61.
410 16. Chen J, Powell D, Hu W-S. High Frequency of Genetic Recombination Is a Common
411 Feature of Primate Lentivirus Replication. Journal of Virology. 2006;80(19):9651.
412 17. Luo B, Cheung HW, Subramanian A, Sharifnia T, Okamoto M, Yang X, et al. Highly parallel
413 identification of essential genes in cancer cells. Proceedings of the National Academy of Sciences.
414 2008;105(51):20380.
415 18. Stein PL, Vogel H, Soriano P. Combined deficiencies of Src, Fyn, and Yes tyrosine kinases
416 in mutant mice. Genes & Development. 1994;8(17):1999-2007.
417 19. Hatzis C, Pusztai L, Valero V, Booser DJ, Esserman L, Lluch A, et al. A Genomic Predictor of
418 Response and Survival Following Taxane-Anthracycline Chemotherapy for Invasive Breast Cancer.
419 JAMA. 2011;305(18):1873-81.
420 20. Ghandi M, Huang FW, Jané-Valbuena J, Kryukov GV, Lo CC, McDonald ER, et al. Next-
421 generation characterization of the Cancer Cell Line Encyclopedia. Nature. 2019;569(7757):503-8.
422 21. Hanke JH, Gardner JP, Dow RL, Changelian PS, Brissette WH, Weringer EJ, et al. Discovery
423 of a Novel, Potent, and Src Family-selective Tyrosine Kinase Inhibitor: STUDY OF Lck- AND FynT-
424 DEPENDENT T CELL ACTIVATION. 1996;271(2):695-701.
425 22. Ianevski A, Giri AK, Aittokallio T. SynergyFinder 3.0: an interactive analysis and consensus
426 interpretation of multi-drug synergies across multiple samples. Nucleic Acids Research.
427 2022;50(W1):W739-W43.
428 23. Kruidenier L, Chung C-w, Cheng Z, Liddle J, Che K, Joberty G, et al. A selective jumonji
429 H3K27 demethylase inhibitor modulates the proinflammatory macrophage response. Nature.
430 2012;488(7411):404-8.

24. Dalvi MP, Wang L, Zhong R, Kollipara RK, Park H, Bayo J, et al. Taxane-Platin-Resistant Lung Cancers Co-develop Hypersensitivity to JumonjiC Demethylase Inhibitors. Cell Reports. 2017;19(8):1669-84.

25. Heinemann B, Nielsen JM, Hudlebusch HR, Lees MJ, Larsen DV, Boesen T, et al. Inhibition of demethylases by GSK-J1/J4. Nature. 2014;514(7520):E1-E2.

26. Sharma SV, Lee DY, Li B, Quinlan MP, Takahashi F, Maheswaran S, et al. A Chromatin-Mediated Reversible Drug-Tolerant State in Cancer Cell Subpopulations. Cell. 2010;141(1):69-80.

27. Hyun K, Jeon J, Park K, Kim J. Writing, erasing and reading histone lysine methylations. Experimental & Molecular Medicine. 2017;49(4):e324-e.

28. Chen YK, Bonaldi T, Cuomo A, Del Rosario JR, Hosfield DJ, Kanouni T, et al. Design of KDM4 Inhibitors with Antiproliferative Effects in Cancer Models. ACS Medicinal Chemistry Letters. 2017;8(8):869-74.

29. Metzger E, Stepputtis SS, Strietz J, Preca B-T, Urban S, Willmann D, et al. KDM4 Inhibition Targets Breast Cancer Stem–like Cells. Cancer Research. 2017;77(21):5900-12.

30. Green TP, Fennell M, Whittaker R, Curwen J, Jacobs V, Allen J, et al. Preclinical anticancer activity of the potent, oral Src inhibitor AZD0530. Molecular Oncology. 2009;3(3):248-61.

31. Gogleva A, Polychronopoulos D, Pfeifer M, Poroshin V, Ughetto M, Martin MJ, et al. Knowledge graph-based recommendation framework identifies drivers of resistance in EGFR mutant non-small cell lung cancer. Nature Communications. 2022;13(1):1667.

32. Hanson SM, Georghiou G, Thakur MK, Miller WT, Rest JS, Chodera JD, et al. What Makes a Kinase Promiscuous for Inhibitors? Cell Chemical Biology. 2019;26(3):390-9.e5.

33. Girotti MR, Pedersen M, Sanchez-Laorden B, Viros A, Turajlic S, Niculescu-Duvaz D, et al. Inhibiting EGF Receptor or SRC Family Kinase Signaling Overcomes BRAF Inhibitor Resistance in Melanoma. Cancer Discovery. 2013;3(2):158-67.

34. Loh Y-H, Zhang W, Chen X, George J, Ng H-H. Jmjd1a and Jmjd2c histone H3 Lys 9 demethylases regulate self-renewal in embryonic stem cells. Genes & Development. 2007;21(20):2545-57.

35. Kim H-Y, Choi H-J, Lee J-Y, Kong G. Cancer Target Gene Screening: a web application for breast cancer target gene screening using multi-omics data analysis. Briefings in Bioinformatics. 2020;21(2):663-75.

36. Sachs N, de Ligt J, Kopper O, Gogola E, Bounova G, Weeber F, et al. A Living Biobank of Breast Cancer Organoids Captures Disease Heterogeneity. Cell. 2018;172(1):373-86.e10.

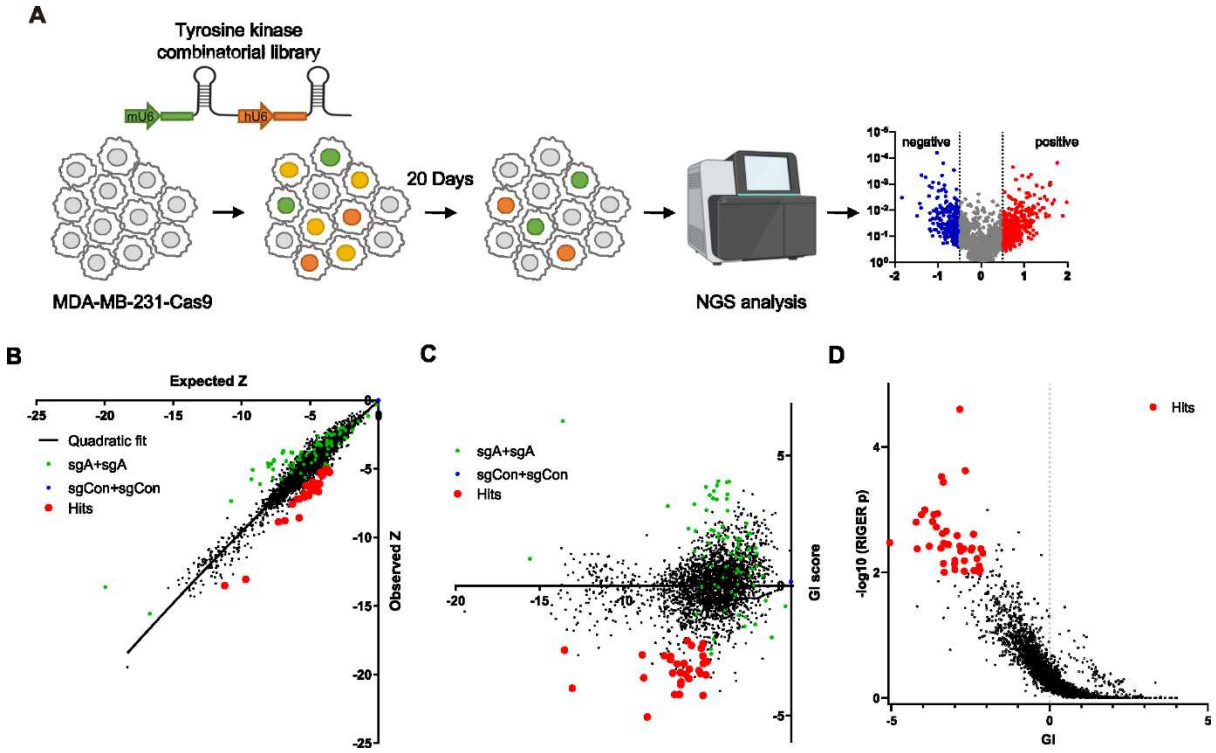

Figure 1. Pairwise CRISPR screen reveals combinations of synthetic lethal tyrosine kinase ablations. (A) Schematic diagram of combinatorial screens performed in TNBC cell line MDA-MB-231. (B) Scatter plot of expected growth phenotype Z score and observed growth phenotype Z score of each gene combination. Green dots indicate gene combinations where the identical gene is targeted by the two sgRNA. Red dots indicate candidate synthetic lethal gene pairs listed in table S1. (C) Scatter plot of growth phenotype Z score and normalized GI score of each gene combination. (D) Scatter plot of gene level GI score and RIGER p value calculated with GI scores of each sgRNA pairs that target the given gene pair.

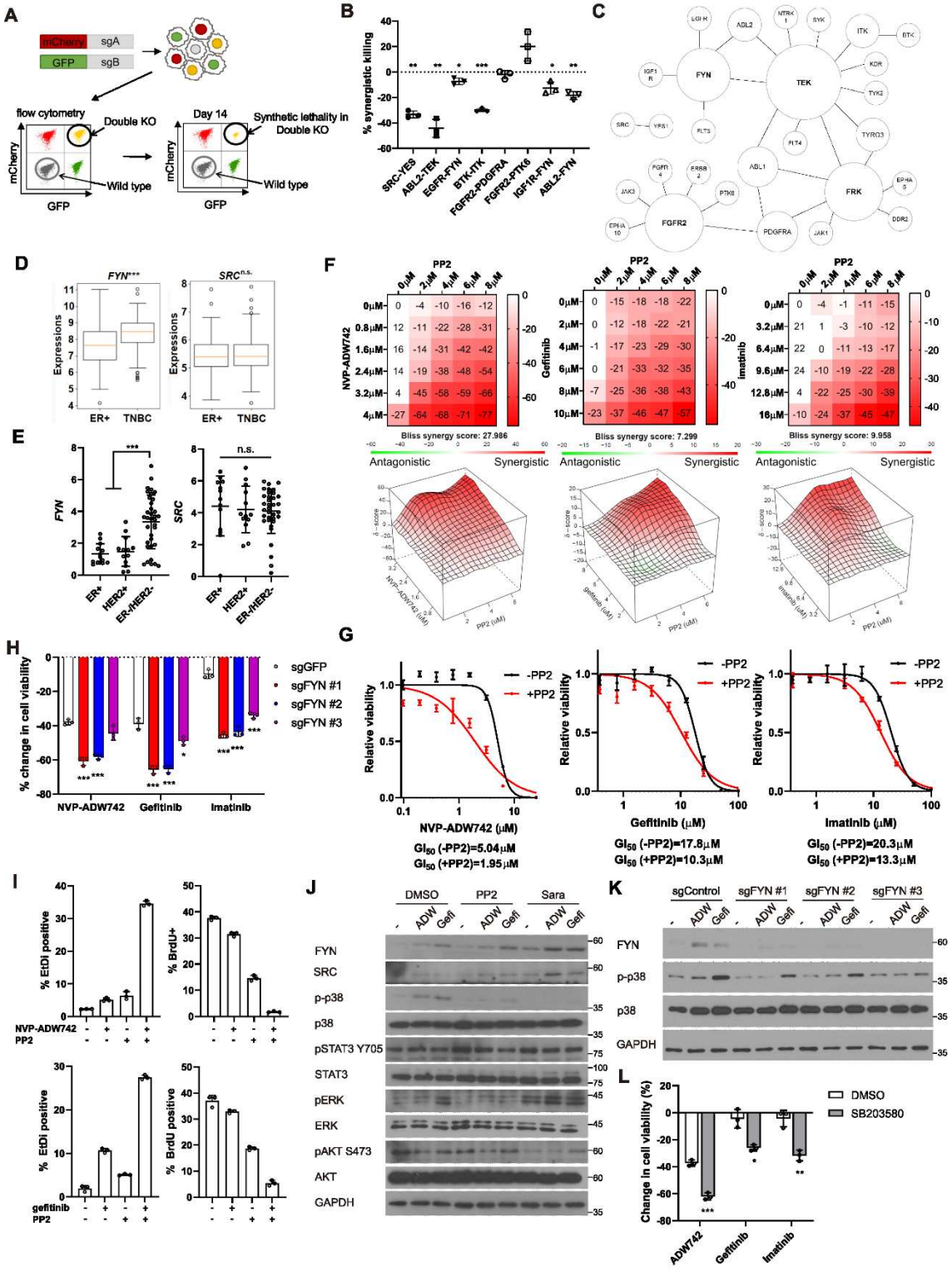

473

474 **Figure 2. FYN is critical mediator of TKI resistance.** (A) Schematic diagram of *in vitro* validation of
475 synthetic lethal gene pairs using sgRNAs. (B) Summary of synergistic killing by sgRNAs targeting indicated
476 gene pairs (n=3). (C) Network analysis of the 30 candidate synthetic lethal gene pairs. The size of each node is

proportional to the number of connections the gene has. (D-E) *FYN* and SRC mRNA expressions in (D) microarray data of primary breast cancers of GSE25066 cohort, and (E) in cancer cell line encyclopedia, for indicated subtypes. (F) Summary of MTT assay with MDA-MB-231 cells treated with the TKI combinations at indicated concentrations (n=2). Synergistic killing is calculated using SynergyFinder with Bliss independence model. (G) Dose response curve of the indicated TKI in the presence and absence of PP2 (n=3). (H) MTT assay with MDA-MB-231 Cas9 cells expressing indicated sgRNAs treated with indicated TKIs (n=3). (I) Cell death and cell proliferation in MDA MB 231 cells treated with NVP-ADW742, gefitinib and PP2 either as single agent or as combination (n=3). (J) western blot analysis of MDA-MB-231 cells treated with indicated drugs. (K) western blot analysis of MDA-MB-231 Cas9 cells expressing indicated sgRNA and treated with indicated drugs. (L) MTT assay of MDA-MB-231 cells treated with indicated drugs (n=3). All data are plotted as mean±s.d. One sample t-test for B, and unpaired two-sided Student's t-test in D,E,H and L. *, $p<0.05$; **, $p<0.01$; ***, $p<0.001$; n.s., $p>0.05$. All replicates are biological replicates.

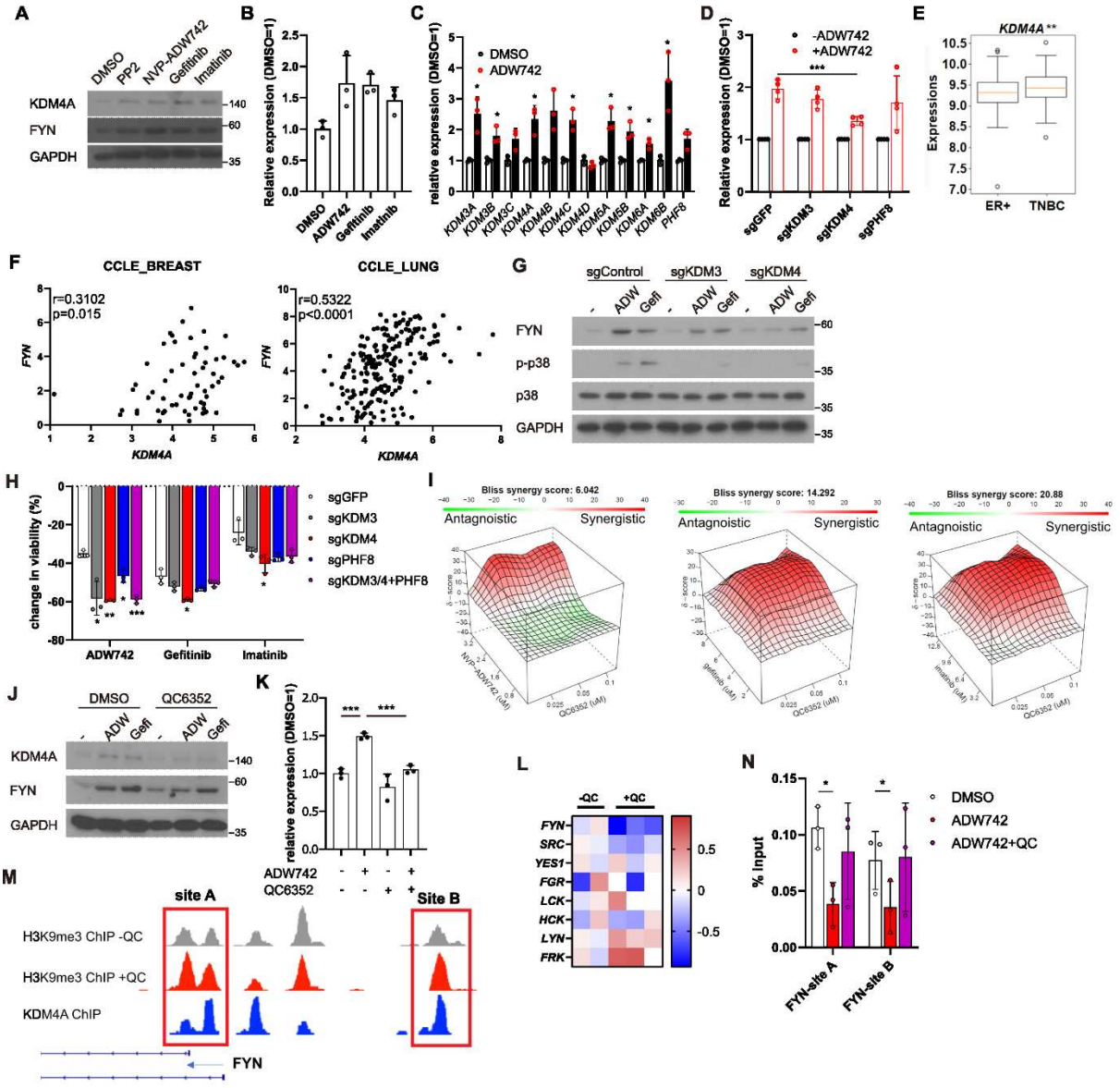

Figure 3. Activation of *KDM4* upregulates *FYN*, conferring drug resistance. (A) Western blot analysis of MDA-MB-231 cells treated with indicated drugs. (B) RT-qPCR analysis of *FYN* expression levels in MDA-MB-231 cells treated with indicated drugs (n=3). (C) RT-qPCR analysis of indicated jumonji family histone demethylase expression levels (n=3). (D) Changes in *FYN* mRNA levels upon NVP-ADW742 treatment in MDA-MB-231 Cas9 cells expressing indicated sgRNAs (n=4). (E) *KDM4A* mRNA levels in primary tumor tissues of indicated subtypes in GSE25066 cohort. (F) Positive correlation of *FYN* and *KDM4A* mRNA levels in CCLE database. (G) western blot analysis of MDA-MB-231 Cas9 cells expressing indicated sgRNA and treated with indicated drugs. (H) MTT assay of MDA-MB-231 Cas9 cells expressing indicated sgRNAs and treated with indicated drugs (n=3). (I) SynergyFinder analysis of MDA-MB-231 cells treated with indicated drug combinations (n=2). (J-K) western blot analysis (J) and RT-qPCR analysis (K) of MDA-MB-231 cells treated

with indicated drugs (n=3). (L) mRNA expression levels of SRC family kinases in breast cancer stem cells treated with QC6352 in RNA sequencing data described in Metzger et. al.(29) (M) H3K9me3 and KDM4A enrichment at genomic locus encoding *FYN* promoter in ChIP sequencing data described in the same study as (L). (N) H3K9me3 Chromatin immunoprecipitation-qPCR analysis of MDA-MB-231 cells treated with indicated drug at specified genomic loci (n=3). All data are plotted as mean±s.d. Unpaired two-sided Student's t-test in B,C,D,E,H and K. Paired two-sided Student's t-test in N. *, p<0.05; **, p<0.01; ***, p<0.001; n.s., p>0.05. All replicates are biological replicates.

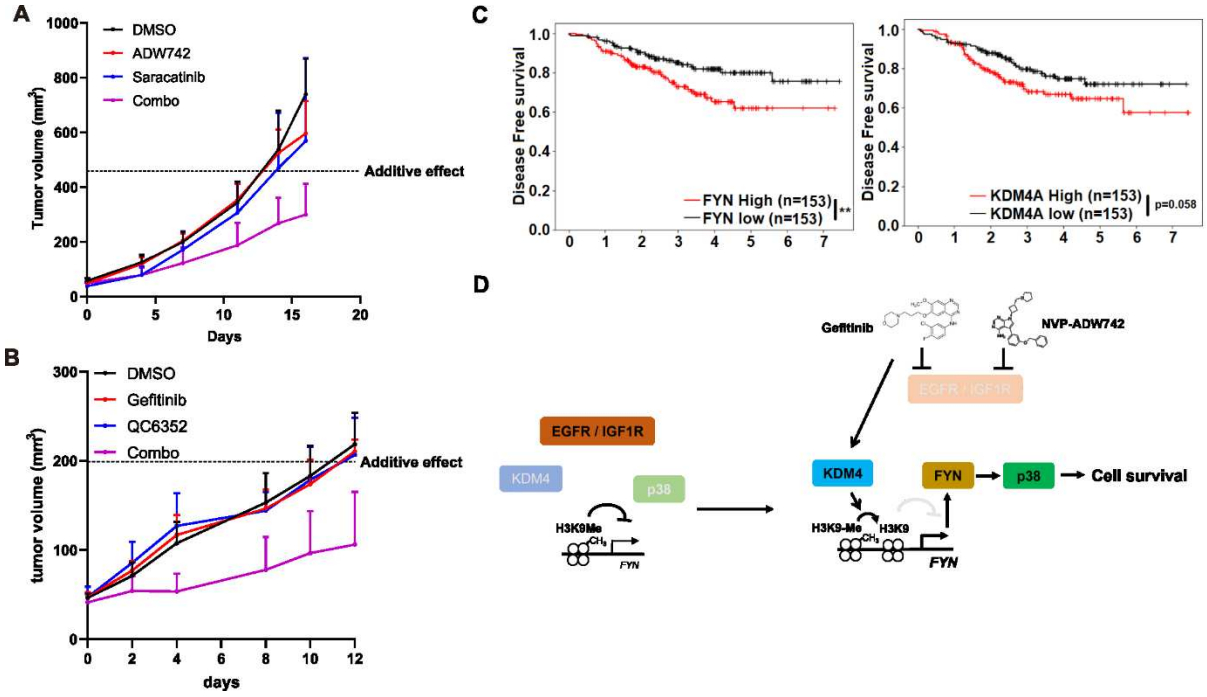

Figure 4. Combination therapy targeting FYN+IGF1R and KDM4+EGFR synergistically eliminates tumor *in vivo*. (A-B) Tumor volume for MDA-MB-231 xenografts treated with indicated drugs. Additive effects were calculated by Bliss independence model (n=5). (C) Distant relapse free survival of GSE25066 patient cohort classified by *FYN* (left) and *KDM4A* (right) mRNA expression. (D) Schematics diagram of the mechanism of KDM4-FYN conferring TKI resistance. All data are plotted as mean±s.d. *, p<0.05; **, p<0.01; ***, p<0.001; n.s., p>0.05. All replicates are biological replicates.

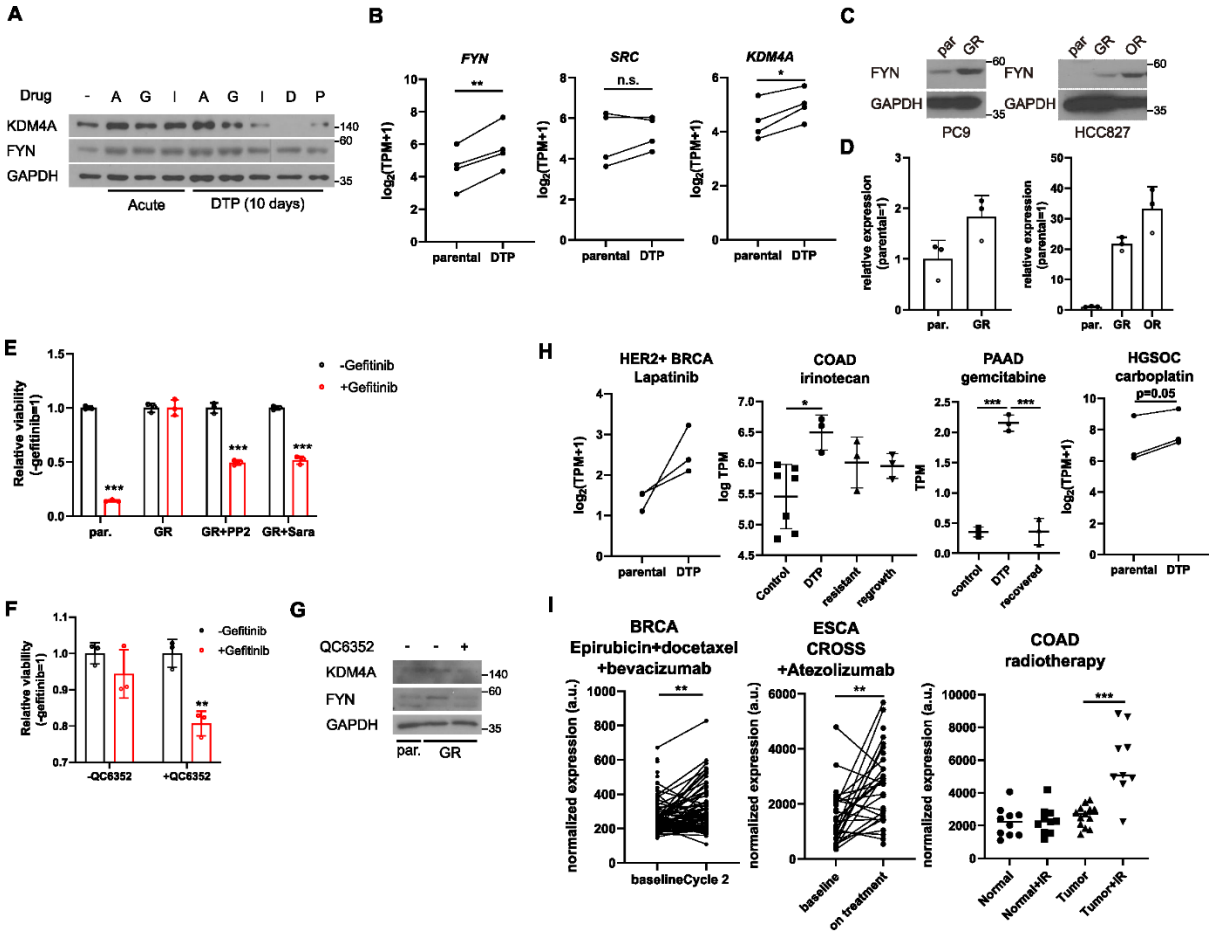

Figure 5. *FYN* and *KDM4* are associated with drug tolerance. (A) MDA-MB-231 cells treated with indicated drugs for short (acute: 2 days) and long (DTP: 10 days) time periods. (B) Summary of mRNA expressions of indicated genes in EGFR mutant lung cancer cells (parental) and their derivative Osimertinib tolerant persisters (DTP). (C-D) western blots (C) and RT-qPCR (D) analyses of indicated parental and EGFR inhibitor resistant lung cancer cells. (E) *FYN* mRNA expression levels of parental and DTP populations in various cancers treated with indicated drugs (n=3). (F) *FYN* mRNA expression levels of residual disease after indicated treatments (n=3). (G-H) MTT assay with PC9 parental (par.) and gefitinib resistant (GR) cells treated with indicated drug combinations. (I) western blot analysis with PC9 cells treated with QC6352. All data are plotted as mean±s.d. Paired two-sided Student's t-test in B, E (HER2+ BRCA set and HGSOC carboplatin set), and F (BRCA set and ESCA set), and unpaired two-sided Student's t-test in E (COAD and PAAD sets) and F (COAD set). *, $p<0.05$; **, $p<0.01$; ***, $p<0.001$; n.s., $p>0.05$. All replicates are biological replicates.